**Supporting Information**

# Sulfur doped ruthenium nanoparticles as a highly efficient electrocatalyst for hydrogen evolution reaction in alkaline media

*Cong Ling,*‡[a] *Hong-Bao Li,*‡[b,*] *Cheng-Zong Yuan,*[a] *Zhengkun Yang,*[b] *Han-Bao Chong,*[a] *Xiao-Jun Qian,*[c] *Xiao-Jie Lu,*[a] *Tuck-Yun Cheang*[d,*] *and An-Wu Xu*[a,*]

[a] Division of Nanomaterials and Chemistry, Hefei National Laboratory for Physical Sciences at the Microscale, University of Science and Technology of China, Hefei, Anhui 230026, People's Republic of China.

[b] Institutes of Physical Science and Information Technology, Key Laboratory of Structure and Functional Regulation of Hybrid Materials, Ministry of Education, Anhui Graphene Engineering Laboratory. Anhui University, Hefei, Anhui, 230601, China.

[c] The First Affiliated Hospital of USTC, Division of Life Sciences and Medicine, University of Science and Technology of China, Hefei, Anhui, 230001, P.R. China.

[d] Scientific Research Center, The First Affiliated Hospital of Guangdong Pharmaceutical University, Guangzhou 510080, China.

*To whom correspondence should be addressed.

Hong-Bao Li; lihb@ahu.edu.cn

Tuck-Yun Cheang; 13631322559@163.com

An-Wu Xu; anwuxu@ustc.edu.cn

‡Cong Ling and Hong-Bao Li contributed equally to this work

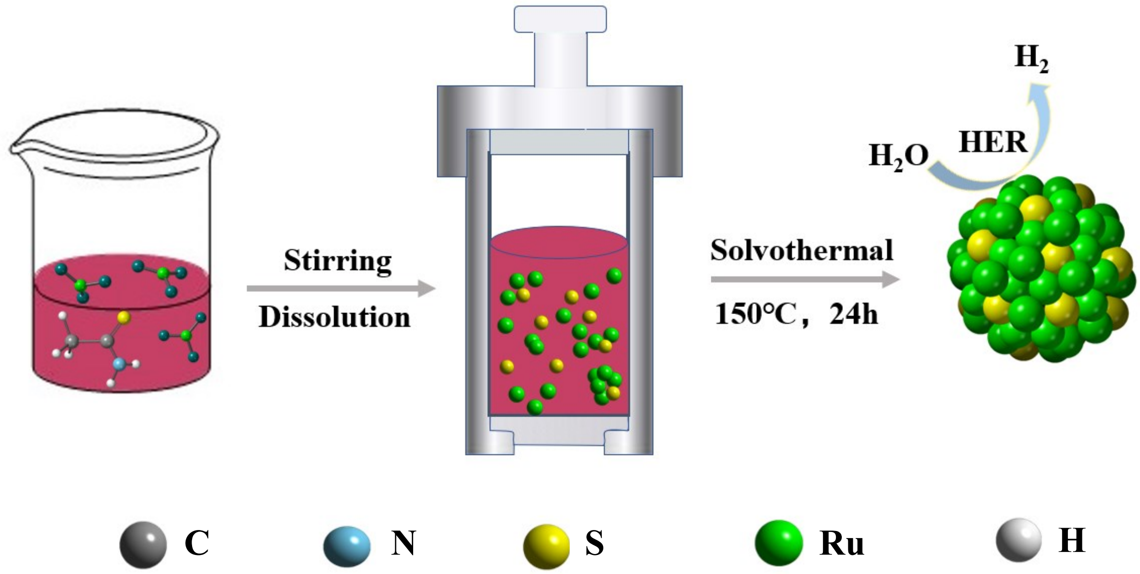


**Scheme S1** Schematic illustration for the synthetic process of Ru-S catalyst.

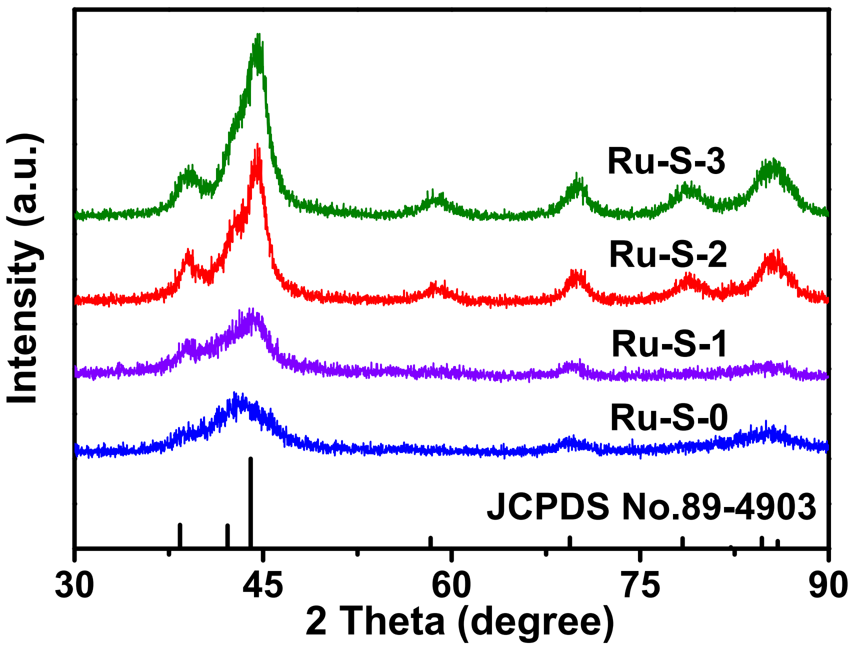


**Fig. S1** The XRD patterns of as-prepared S-doped ruthenium catalysts. It shows that catalysts with different sulfur-content have the same diffraction peaks. The diffraction peaks can be assigned to Ru with hexagonal phase (JCPDS No. 89-4903).

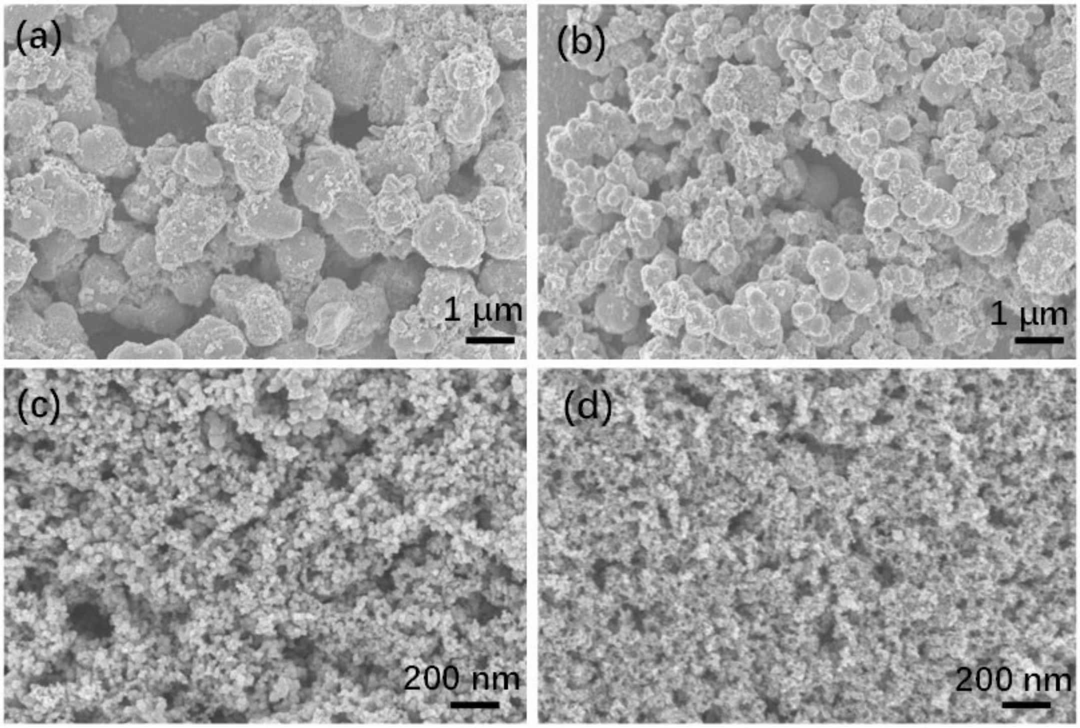


**Fig. S2** The SEM images of as-prepared different sulfur-content catalysts, (a) Ru-S-0, (b) Ru-S-1, (c) Ru-S-2, and (d) Ru-S-3. These samples have a quite uniform morphology with different particle size.

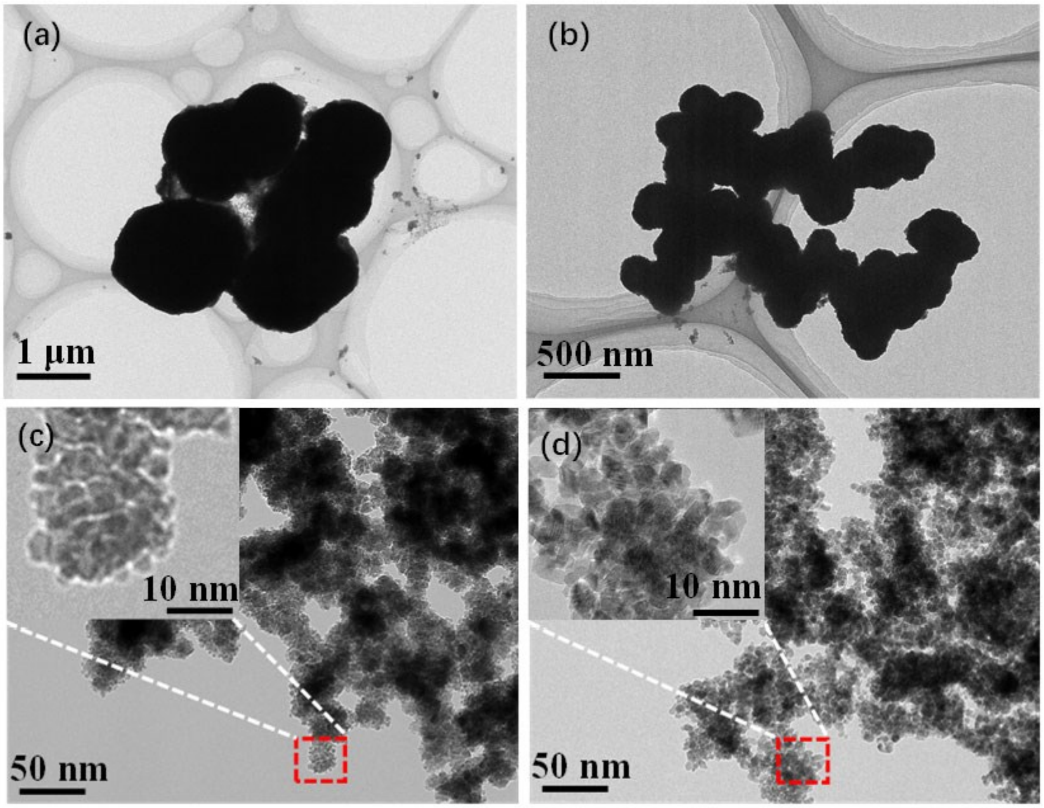


**Fig. S3** The TEM images of as-prepared different sulfur-content catalysts, (a) Ru-S-0, (b) Ru-S-1, (c) Ru-S-2 (inset: HR-TEM images), and (d) Ru-S-3 (inset: HR-TEM images).

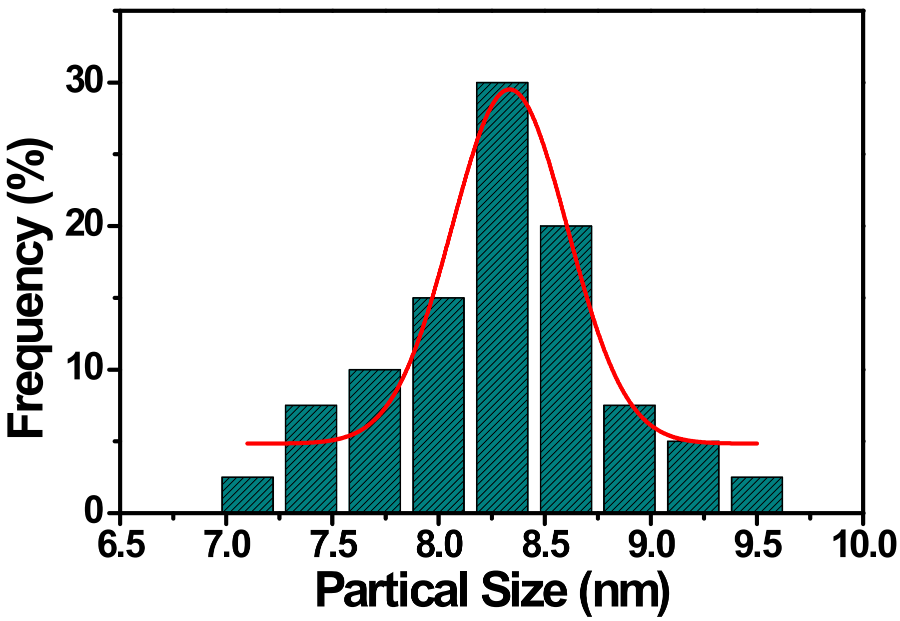


**Fig. S4** Particle size distribution of as-prepared Ru-S-2 catalyst. It possessed crystal size of 8.3 nm in average diameter.

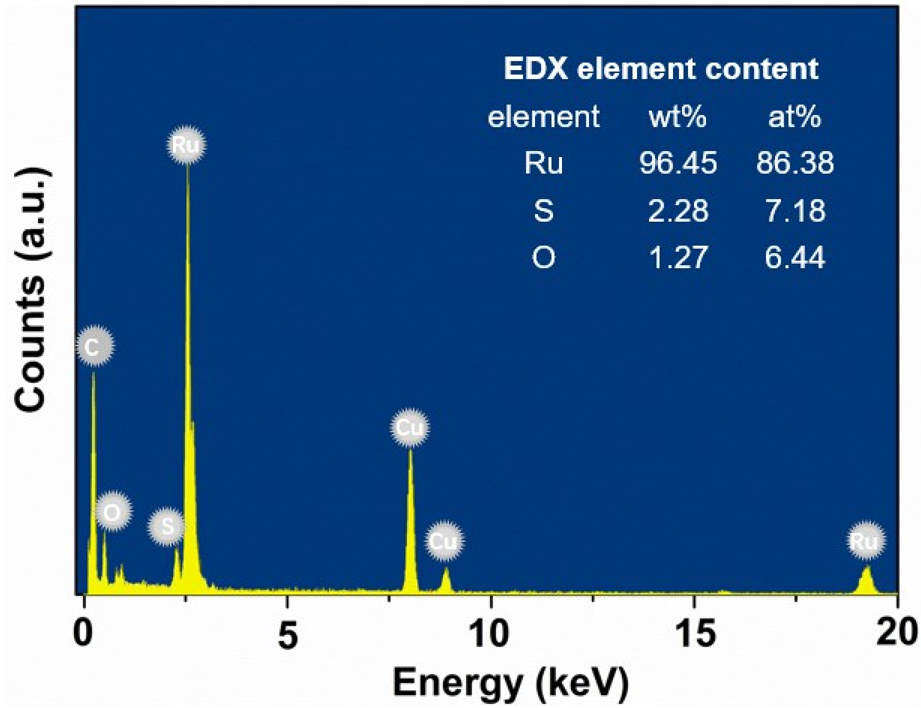


**Fig. S5** EDS spectrum of as-prepared Ru-S-2 catalyst, and the corresponding elemental content of Ru, S, O.

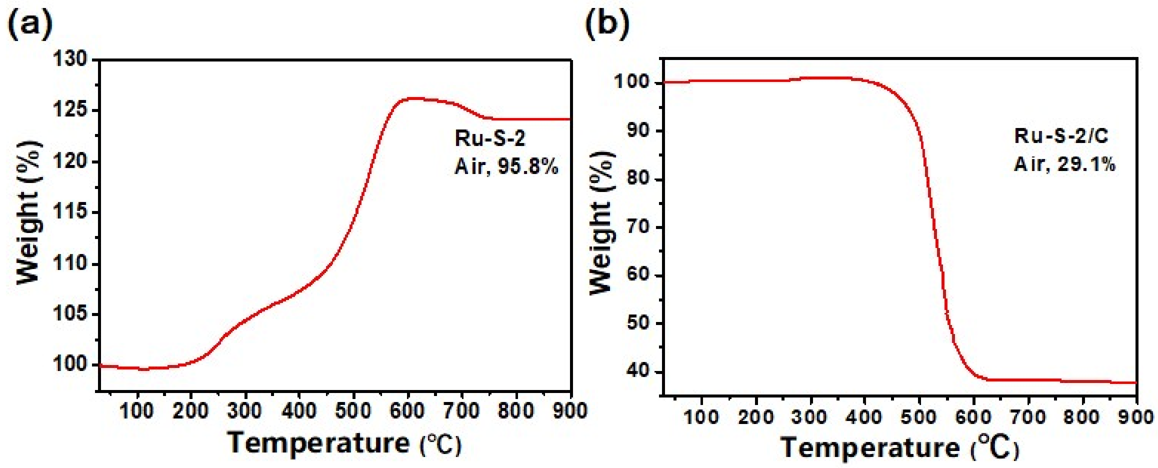


**Fig. S6** (a), and (b) are TGA curves of as-prepared Ru-S-2 and Ru-S-2/C catalysts at atmosphere with a ramping rate of 10 ℃ $min^{-1}$, respectively. The residue is pure $RuO_2$ metal.

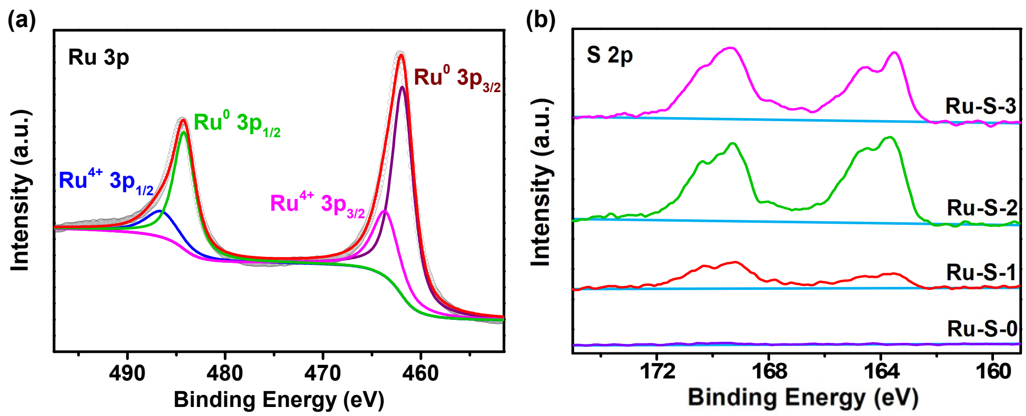


**Fig. S7** (a) Ru 3p spectra of Ru-S-2 and (b) S 2p XPS spectra of as-prepared serial S-doped catalyst. Figure (b) showed that Ru-S-2 possessed the highest sulfur content.

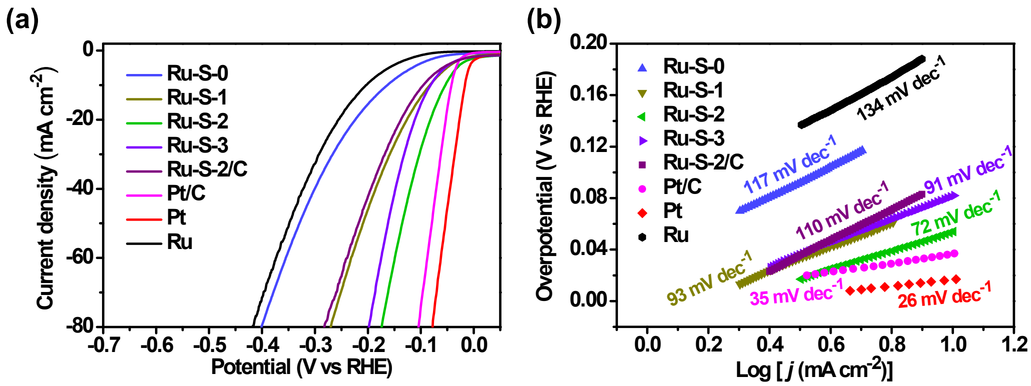


**Fig. S8** (a) The linear sweep voltammetry (LSV) curves and (b) Tafel curves were obtained over as-prepared catalysts in $N_2$-saturated 0.5 M $H_2SO_4$ solution. The LSV curves and Tafel curves exhibited obvious activity in acidic media.

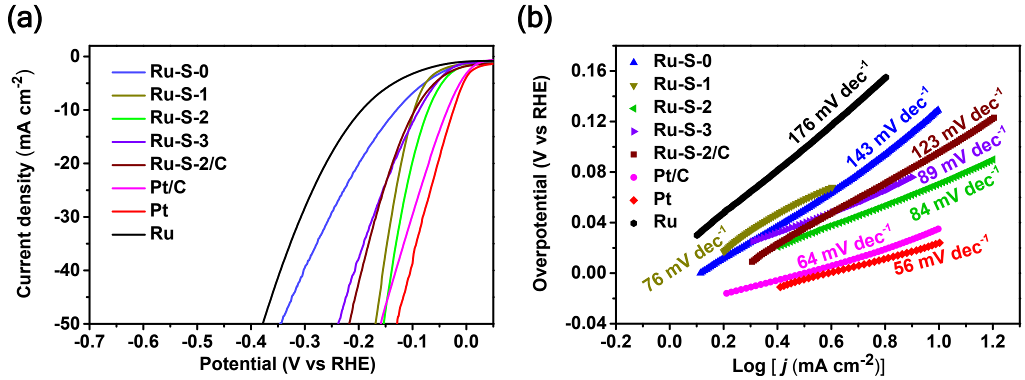


**Fig. S9** (a) The linear sweep voltammetry (LSV) curves and (b) Tafel curves were obtained over as-prepared catalysts in $N_2$-saturated 1 M PBS solution. The LSV curves and Tafel curves exhibited obvious activity in the neutral system.

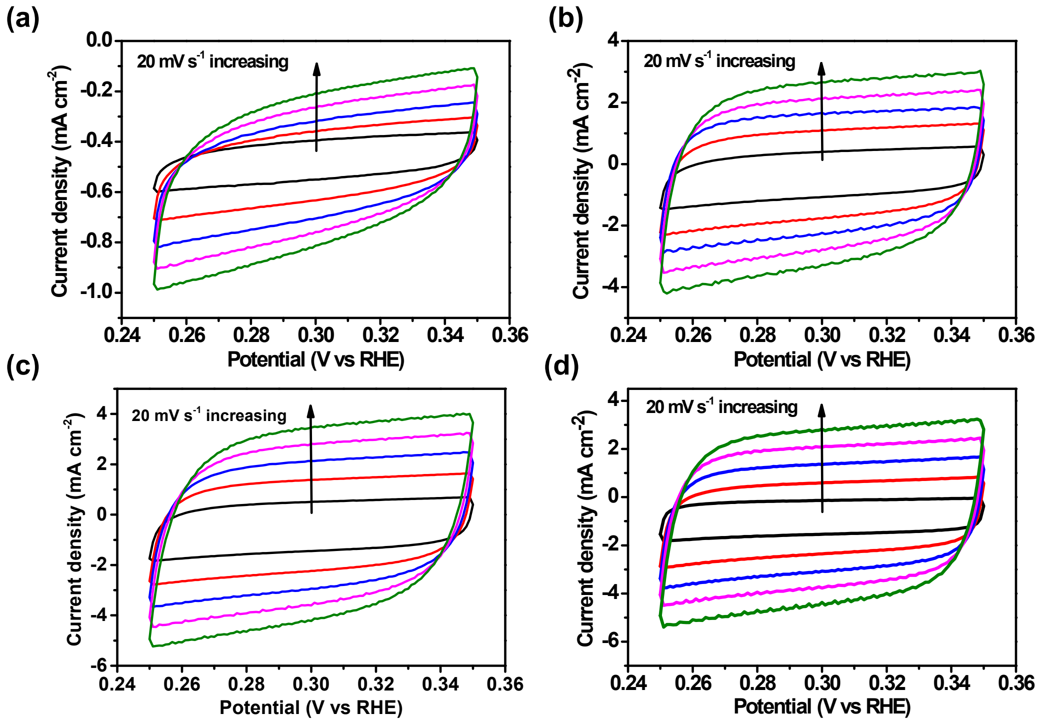


**Fig. S10** CV curves of as-prepared S-doped ruthenium catalysts 1.0 M KOH, (a) Ru-S-0, (b) Ru-S-1, (c) Ru-S-2, (d) Ru-S-3.

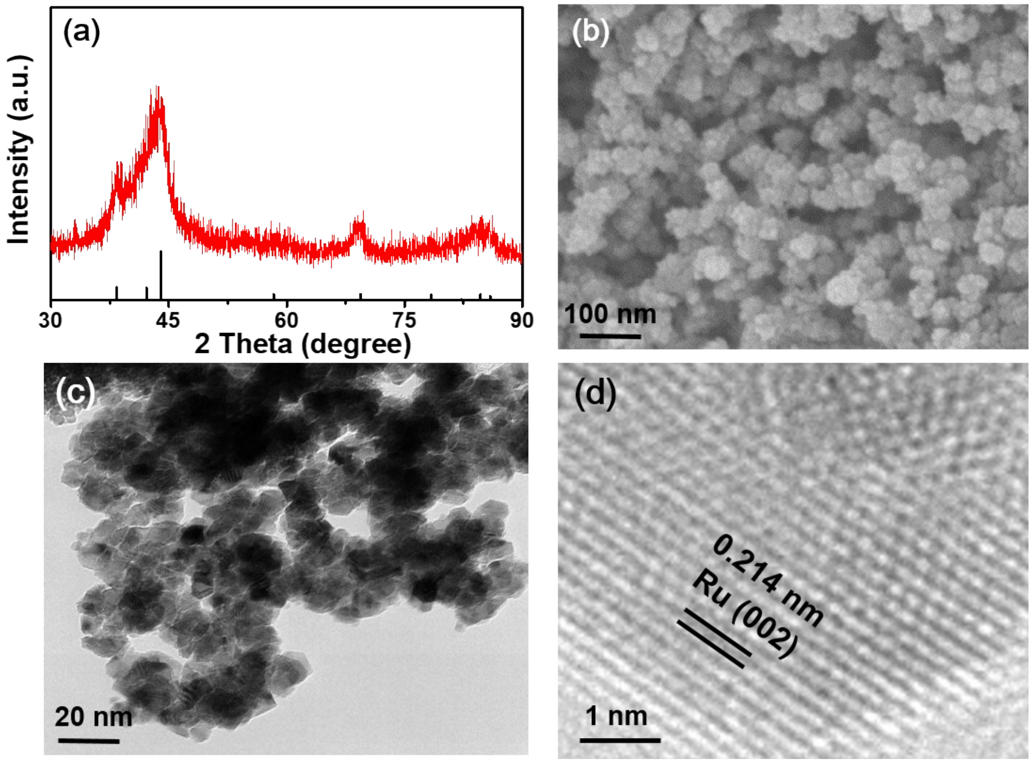


**Fig. S11** (a) The XRD pattern, (b) SEM, (c) TEM, and (d) HRTEM images of Ru-S-2 catalysts after 12 h electrocatalysis for HER in 1.0 M KOH solution.

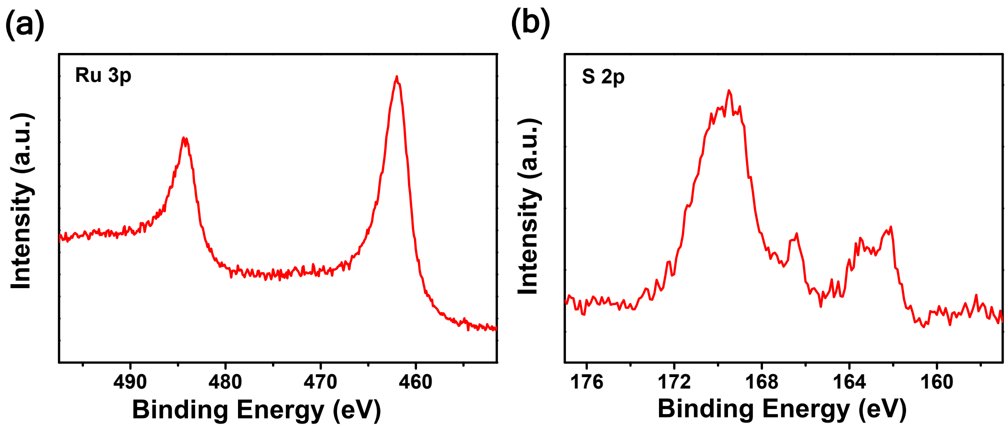


**Fig. S12** (a) Ru 3p, and (b) S 2p XPS spectra of as-prepared Ru-S-2 catalyst after 12 h electrocatalysis for HER in 1.0 M KOH solution.

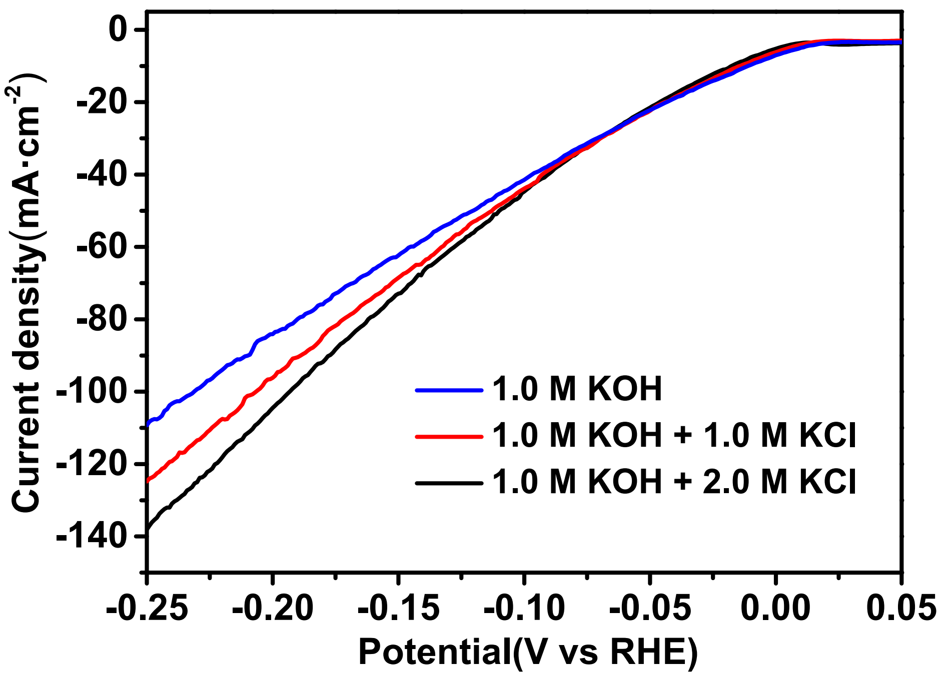


**Fig. S13** HER polarization curves of Ru-S-2 catalyst in pH of 14 with different concentrations of $K^+$. The result showed that the activities of Ru-S-2 increased with the addition of $K^+$ at high current density.

**Table S1.** Summary of some recently reported representative HER electrocatalysts in alkaline electrolytes.

| Catalyst | η (@ 10 mA $cm^{-2}$) | Tafel Slope (mV $dec^{-1}$) | Electrolyte | References |
|---|---|---|---|---|
| **Ru-S-2** | **10** | **53** | **1 M KOH** | **This work** |
| **Ru-S-2/C** | **40** | **56** | **1 M KOH** | **This work** |
| R-$TiO_2$: Ru | 150 | 95 | 0.1 M KOH | J. Am. Chem. Soc., 2018, 140, 5719. |
| $RuP_2$@NPC | ~52 | 69 | 1 M KOH | Angew. Chem. Int. Ed., 2017, 56, 11559. |
| Ru@$C_2N$ | 17 | 38 | 1 M KOH | Nat. Nanotech., 2017, 12, 441. |
| Ru/$C_3N_4$/C | 79 | 69 | 0.1 M KOH | J. Am. Chem. Soc., 2016, 138, 16174. |
| RuSi | 37 | - | 1 M KOH | Angew. Chem. Int. Ed., 2019, 58, 11409. |
| Ru-$MoO_2$ | 29 | 44 | 1 M KOH | J. Mater. Chem. A., 2017, 5, 5474. |
| RuCo@NC | 28 | 31 | 1 M KOH | Nat. Commun., 2017, 8, 14969. |
| Ru@CN | 50 | - | 0.1 M KOH | Energy Environ. Sci., 2018, 11, 800. |
| $Co(OH)_2$/Pt (111) | ~248 | - | 1 M KOH | Nat. Mater., 2012, 11, 550. |
| Pt3Ni/NiS | ~45 | - | 0.1 M KOH | Nat. Commun., 2017, 8, 14580. |
| Ni-BDT-A | 80 | 70 | 1 M KOH | Chem., 2017, 3, 122. |
| PtNi | 65 | 74 | 0.1 M KOH | Nat. Commun., 2017, 8, 15131. |
| NiS/$MoS_2$/C | 117 | 58 | 1 M KOH | Electrochim. Acta., 2018, 274, 74. |

| | | | | |
|---|---|---|---|---|
| $Ni_2P$/Ni/NF | 98 | 72 | 1 M KOH | ACS Catal., 2015, 6, 714. |

**Table S2.** Summary of some recently reported representative HER electrocatalysts in acidic electrolytes.

| Catalyst | η (@ 10 mA $cm^{-2}$) | Tafel Slope (mV $dec^{-1}$) | Electrolyte | References |
|---|---|---|---|---|
| **Ru-S-2** | **54** | **72** | **0.5 M $H_2SO_4$** | **This work** |
| **Ru-S-2/C** | **95** | **110** | **0.5 M $H_2SO_4$** | **This work** |
| Ru@CN | 126 | - | 0.5 M $H_2SO_4$ | Energy Environ. Sci., 2018, 11, 800. |
| RuP@NPC | 125 | 107 | 0.5 M $H_2SO_4$ | Adv. Energy Mater., 2018, 8, 1870130. |
| Pt MLAg NF/Ni foam | ~70 | 53 | 0.5 M $H_2SO_4$ | Sci. Adv., 2015, 1, 1400268. |
| $CoN_x$/C | 133 | 57 | 0.5 M $H_2SO_4$ | Nat. Commun., 2015, 6, 7992. |
| CoPS film | 128 | 57 | 0.5 M $H_2SO_4$ | Nat. Mater., 2015, 14, 1245. |
| M-$MoS_2$ | 175 | 41 | 0.5 M $H_2SO_4$ | Nat. Commun., 2016, 7, 10672. |
| mPF-$MoS_2$ | 195 | - | 0.5 M $H_2SO_4$ | Nat. Commun., 2017, 8, 14430. |
| SV-$MoS_2$ | 170 | 60 | 0.5 M $H_2SO_4$ | Nat. Mater., 2016, 15, 364. |
| $CoMoS_x$ | ~207 | - | 0.1 M $H_2SO_4$ | Nat. Mater., 2016, 15, 197. |
| Co-NG | 147 | 82 | 0.5 M $H_2SO_4$ | Nat. Commun., 2015, 6, 8668. |

**Table S3.** Comparison of electrochemical surface areas (ECSA) and catalytic activities of Ru catalysts at different sulfur content.

| Catalyst | $C_{dl}$ ($mF\ cm^{-2}$) | $C_{DL}$ (mF) | ECSA ($cm^2$) | $J_{\eta = 100\ mV}$ (mA) | RF |
|---|---|---|---|---|---|
| Ru-S-0 | 1.85 | 0.35 | 8.75 | 1.65 | 45 |
| Ru-S-1 | 27.73 | 5.44 | 138 | 4.68 | 704 |
| Ru-S-2 | 40.17 | 7.87 | 197 | 10.1 | 1005 |
| Ru-S-3 | 37.01 | 7.25 | 181 | 4.98 | 923 |

$C_{DL} = C_{dl} * 0.196\ cm^2$, $ECSA = C_{DL}/C_s$, $C_s = 0.04\ mF\ cm^{-2}$, $J_{\eta=100\ mV}$ represents the current obtained at overpotential of 100 mV, RF = ECSA/0.196 $cm^2$.

**Table S4.** The absorption energy ($E_{abs}$, in eV) and dissociation energies ($E_{dis}$, in eV) of the $H_2O$ on different surfaces: Pt (111), Ru (001), Ru-S + $Ru_{site}$ and Ru-S + $S_{site}$ and the distance (in Å) of the weak interaction between oxygen atom (O) and the mental atom (Pt or Ru).

| | Pt (111) | Ru (001) | Ru-S+ $Ru_{site}$ | Ru-S + $S_{site}$ |
|---|---|---|---|---|
| $E_{ads}$(eV) | -0.22 | -0.40 | -0.41 | -0.52 |
| O-Pt/Ru（Å） | 2.42 | 2.33 | 2.32 | 2.30 |
| $E_{dis}$ (eV) | 3.47 | 2.92 | 2.50 | 2.38 |

**Table S5.** Distance (in Å) between different Ru atoms and between the X atom (X= S, Se, Te) and its surrounding metal atoms.

| | Ru | Ru-S | Ru-Se | Ru-Te |
|---|---|---|---|---|
| Ru-Ru（Å） | 2.71 | 2.69 | 2.68 | 2.68 |
| Ru-X（Å） | -- | 2.76 | 2.78 | 2.78 |